We have already obtained the following values: $x_0=1$, $y_0=0$; $x_1=1$, $y_1=\frac{1}{2}$; $x_2=\frac{7}{8}$, $y_2=\frac{1}{2}$. We will now show that

$$\lim_{\nu=\infty} x_\nu = \lim_{\nu=\infty} y_\nu = 1/(2)^{1/2},$$

which indicates a poor convergence.

To prove this, we note that the products

$$\langle 0 \mid (b_\beta a_n)(b_\alpha a_m)(a_m^\dagger b_\alpha^\dagger)(a_n^\dagger b_\beta^\dagger) \mid 0\rangle = 1$$

and

$$\langle 0 \mid (b_\beta a_m)(b_\alpha a_n)(a_m^\dagger b_\alpha^\dagger)(a_n^\dagger b_\beta^\dagger) \mid 0\rangle = -1$$

may be calculated with the help of the commutation relations for the particle-hole operators. However, those scalar products may also be calculated by making use of the expansions for $(a_m^\dagger b_\alpha^\dagger)(a_n^\dagger b_\beta^\dagger)$ and $(a_m^\dagger b_\beta^\dagger)(a_n^\dagger b_\alpha^\dagger)$. One then finds

$$x_\infty^2 + y_\infty^2 = 1,$$
$$2x_\infty y_\infty = 1,$$

so that

$$x_\infty = y_\infty = 1/(2)^{1/2}.$$

As an example of the speed of convergence for a physically interesting quantity, we consider the second-order energy. Disregarding consistency, we obtain

$$E_\nu^{(2)} = \tfrac{1}{2}(x_\nu^2+y_\nu^2) \sum_{\alpha\beta mn} \frac{V_{\alpha\beta,mn}V_{mn,\alpha\beta}}{\epsilon_\alpha+\epsilon_\beta-\epsilon_m-\epsilon_n} - \tfrac{1}{2}(2x_\nu y_\nu) \sum_{\alpha\beta mn} \frac{V_{\alpha\beta,mn}V_{mn,\beta\alpha}}{\epsilon_\alpha+\epsilon_\beta-\epsilon_m-\epsilon_n}$$

and it happens that even for $\nu=2$ both $(x_\nu^2+y_\nu^2)$ and $2x_\nu y_\nu$ are already quite near 1, although the equality is only attained for $\nu=\infty$. We remark finally that the relation

$$a_m^\dagger b_\alpha^\dagger a_n^\dagger b_\beta^\dagger \mid 0\rangle = [1/(2)^{1/2}](B_{m\alpha}^\dagger B_{n\beta}^\dagger - B_{m\beta}^\dagger B_{n\alpha}^\dagger) \mid 0\rangle,$$

arising in an infinite order Beliaev-Zelevinsky expansion, is contained in Marumori's prescription[7] for mapping a many-fermion Hilbert space into a many-boson Hilbert space.

[7] T. Marumori, M. Yamamura, and A. Tokunaga, Progr. Theoret. Phys. (Kyoto) **31**, 1009 (1964).

PHYSICAL REVIEW C VOLUME 1, NUMBER 3 MARCH 1970

Excitation of $T=1$ Particle-Hole States in C^{12} by Inelastic Electron Scattering*

T. W. DONNELLY†

Institute of Theoretical Physics, Department of Physics, Stanford University, Stanford, California 94305

(Received 17 June 1969)

The $T=1$ single-particle-hole states of C^{12} are considered on the basis of the harmonic-oscillator shell model in the particle-hole formalism developed by Lewis and Walecka. Configuration mixing is included via a Serber-Yukawa residual interaction. Resulting mixed states lying close in energy are grouped together into complexes whose inelastic-electron-scattering form factors are then compared with recent experimental data. This comparison is done mainly at large momentum transfers and large scattering angles, where the transverse excitations (and consequently the $T=1$ states) dominate, and where the excitation spectrum contains only a few strongly excited features (to be related here to collective single-particle-hole states). By working at high momentum transfer, the contributions from transitions of high multipolarity can be strongly enhanced. Here all possible $T=1$ single-particle-hole states of all allowed angular momenta are considered in a basis including single-particle states up to the $2s$-$1d$ shell. A simple square-well shell model is used to account for the quasielastic cross section in the giant-resonance region. All of the gross features of the experimental excitation spectrum for excitation energies between 14 and 30 MeV can be accounted for on the basis of this simple model.

I. INTRODUCTION

INELASTIC electron scattering provides a powerful means for obtaining information about the charge and current distributions of nuclei. For an excitation at a given energy loss, data taken as a function of three-momentum transfer, in principle, provide the Fourier transforms of the charge and current distributions, i.e., provide the inelastic form factors. In practice, some model for the nucleus is generally used to provide the nuclear four-current and the resulting model form factors are compared with experiment.[1,2] By working at large electron scattering angles, where the strongly angle-dependent $\tan^2(\frac{1}{2}\theta)$ factor in the cross section becomes large, states excited by transverse multipoles can be enhanced over longitudinal excitations. The transition operators for electron scattering contain isoscalar and isovector terms and consequently allow only states of $T=0$ and $T=1$, respectively, to be

* Research sponsored by the Air Force Office of Scientific Research, Office of Aerospace Research, U.S. Air Force under AFOSR Contract No. F44620-68-C-0075.

† National Research Council of Canada Postdoctoral Fellow. Present address: Department of Physics, University of Toronto, Toronto 181, Ontario, Canada.

[1] R. Hofstadter, Ann. Rev. Nucl. Sci. **7**, 231 (1957).

[2] T. deForest, Jr., and J. D. Walecka, Advan. Phys. **15**, 1 (1966).

reached from a $T=0$ initial state such as the ground state of C^{12}. Since the isovector magnetic moment $\mu_V=\mu_p-\mu_n=4.71\mu_N$ which occurs in the transverse form factor is large compared to the isoscalar magnetic moment $\mu_S=\mu_p+\mu_n=0.88\mu_N$, the $T=1$ excited states in C^{12} are expected to dominate over the $T=0$ states when the transverse form factors are the most important, viz., at large angles. In the present work,[3] where comparison is made primarily with data taken at large angles, only the $T=1$ excitations are considered.

At large values of three-momentum transfer q, where the long-wavelength approximation is not valid, states of high angular momentum become as important as those excited by the lowest multipole possible. It should be emphasized that inelastic electron scattering provides *one of the few ways* of extensively studying these states: By working at high momentum transfer where the excitation spectrum is relatively simple, containing only a few strongly excited features, one can obtain information about the collective single-particle-hole nature of the states. In particular, states of high angular momentum can be strongly excited at large q. Here comparison is made with data taken over a large range of momentum transfer and the inclusion of all multipole transitions allowed proves to be vital.

Since in electron scattering the transition operators are one-body operators, i.e., simply sums of single-particle operators, the states expected to be most strongly excited from closed-shell nuclei are linear combinations of pure single-particle-hole states. To the extent that C^{12} can be considered to have closed $1s_{1/2}$ and $1p_{3/2}$ shells, the simplest structure observed in electron scattering should be composed of groupings of these collective single-particle-hole excitations. Indeed, if the inelastic excitation function is averaged over energy intervals of the order of 1 MeV, one expects to find features remaining which can be ascribed to the single-particle-hole structure of the excitation. This averaging procedure corresponds to looking at excitations in the nucleus that take place over a relatively short time, before decaying into the more complicated states which correspond to the fine structure observed. These averaged complexes of single-particle-hole states are then the "doorway" states[4,5] for inelastic electron scattering. In fact, large well-defined peaks are observed[3] when inelastic-electron-scattering data are averaged over energy intervals of the order of 1 MeV. In studies with higher resolution, one would expect to see (and does see) additional structure corresponding to collision admixtures of more complicated many-particle–many-hole states.

In the present work, the dominant $T=1$ single-particle-hole states of C^{12} are considered in detail within the framework of the harmonic-oscillator shell model. The single-particle-hole formalism of Lewis and Walecka[6] is used in describing the excited states of C^{12}, where the ground state is taken to have closed $1s_{1/2}$ and $1p_{3/2}$ shells. The Hamiltonian is diagonalized in the space of such states in the presence of a Serber-Yukawa residual interaction (obtained from a fit to low-energy n-p scattering data).[7] The resulting energy spectrum is used, together with experimental information on the location of known levels, in grouping the single-particle-hole states into complexes whose form factors are subsequently compared with experimental form factors.[8–20] This provides an interpretation of the gross-structure form factors in terms of form factors for groupings of single-particle-hole states. In Sec. II, the formalism presented in Lewis and Walecka[6] and in deForest and Walecka[2] is reviewed. Section III contains the resulting energy spectrum and form factors, and Sec. IV is a discussion of these results. Finally, an Appendix is included which contains expressions for the pertinent form factors as functions of momentum transfer.

II. FORMALISM

The formalism for the single-particle-hole states considered in detail by Lewis and Walecka (LW)[6] is briefly reviewed here. LW considered linear combinations of particle-hole states of given angular momentum J and isospin T

$$\Psi_{JM_JTM_T}(1\cdots A)=\sum_K \alpha_{JT}{}^K\Phi_{JM_JTM_T}{}^K(1\cdots A), \quad (1)$$

where K stands for the particle-hole quantum numbers $(n_1l_1j_1)(n_2l_2j_2)^{-1}$, with labels 1 for particles and 2 for holes. The Φ's are the pure particle-hole states given by

[3] A preliminary account of this work (referred to as I), with the experimental results of I. Sick and E. B. Hughes, has previously been reported [T. W. Donnelly, J. D. Walecka, I. Sick, and E. B. Hughes, Phys. Rev. Letters **21,** 1196 (1968)].

[4] H. Feshbach, in *Proceedings of the International Nuclear Physics Conference, Gatlinburg, Tennessee, 1966*, edited by R. L. Becker and A. Zucker (Academic Press Inc., New York, 1967), p. 181.

[5] H. Feshbach, A. K. Kerman, and R. H. Lemmer, Ann. Phys. (N.Y.) **41,** 230 (1967).

[6] F. H. Lewis, Jr., and J. D. Walecka, Phys. Rev. **133,** B849 (1964).

[7] J. F. Dawson, I. Talmi, and J. D. Walecka, Ann. Phys. (N.Y.) **18,** 339 (1962).

[8] G. A. Proca and D. B. Isabelle, Nucl. Phys. **A109,** 177 (1968).

[9] G. R. Bishop and A. Bottino, Phys. Letters **10,** 308 (1964).

[10] B. Dudelzak and R. E. Taylor, J. Phys. Radium **22,** 544 (1961).

[11] W. C. Barber, F. Berthold, G. Fricke, and F. E. Gudden, Phys. Rev. **120,** 2081 (1960).

[12] F. Gudden, Phys. Letters **10,** 313 (1964).

[13] H. Schmid and W. Scholz, Z. Physik **175,** 430 (1963).

[14] G. R. Bishop, Phys. Rev. Letters **19,** 659 (1967).

[15] T. deForest, Jr., J. D. Walecka, G. Vanpraet, and W. C. Barber, Phys. Letters **16,** 311 (1965).

[16] G. A. Beer, T. E. Drake, R. M. Hutcheon, V. W. Stobie, and H. S. Caplan, Nuovo Cimento **53B,** 319 (1968).

[17] J. Goldemberg and W. C. Barber, Phys. Rev. **134,** B963 (1964).

[18] H. Crannell, H. A. Dahl, and F. H. Lewis, Jr., Phys. Rev. **155,** 1062 (1967).

[19] G. Ricco, H. S. Caplan, R. M. Hutcheon, and R. Malvano, Nucl. Phys. **A114,** 685 (1968).

[20] J. Goldemberg, W. C. Barber, F. H. Lewis, Jr., and J. D. Walecka, Phys. Rev. **134,** B1022 (1964).

LW. Inserting these linear combinations into the Schrödinger equation and using the orthonormality properties of the Φ's gives the secular equation

$$\sum_K [(\Phi_{JM_JTM_T}{}^{K'} \mid H \mid \Phi_{JM_JTM_T}{}^{K}) - E\delta_{K'K}]\alpha_{JT}{}^{K}=0, \quad (2)$$

which can be diagonalized to yield the energy eigenvalues E and coefficients $\alpha_{JT}{}^{K}$. LW show that

$$(\Phi_{JM_JTM_T}{}^{K'} \mid H \mid \Phi_{JM_JTM_T}{}^{K}) = \delta_{K'K}E_0(K) + (K', JM_JTM_T \mid v(1,2) \mid K, JM_JTM_T), \quad (3)$$

where $E_0(K)$ is the unperturbed energy of the particle-hole pair K, obtained from energies in nuclei with $A\pm1$ particles. The potential $v(1, 2)$ is a nonsingular potential which is obtained by fitting low-energy nucleon-nucleon scattering data.

Assuming the spin dependence can be factored out,

$$v(1,2)=V(r_{12})\cdot\sigma(1,2), \quad (4)$$

the matrix elements of the potential for $T=1$ states, using harmonic-oscillator radial wave functions, are given by

$$(K', JM_JTM_T \mid v(1,2) \mid K, JM_JTM_T) = -[j_1'][j_2'][j_1][j_2]\sum_{\bar{J}LS} \begin{Bmatrix} j_1 & j_2 & J \\ j_1' & j_2' & \bar{J} \end{Bmatrix} \begin{Bmatrix} l_1' & l_2 & L \\ \frac{1}{2} & \frac{1}{2} & S \\ j_1' & j_2 & \bar{J} \end{Bmatrix} \begin{Bmatrix} l_1 & l_2' & L \\ \frac{1}{2} & \frac{1}{2} & S \\ j_1 & j_2' & \bar{J} \end{Bmatrix} ([\bar{J}][L][S])^2 \times \frac{((\frac{1}{2}\frac{1}{2})S \,||\, \sigma(1,2) \,||\, (\frac{1}{2}\frac{1}{2})S)}{[S]} \sum_p C(n_1'l_1'n_2l_2; n_1l_1n_2'l_2'; L, p) I_p(V), \quad (5)$$

where $[l]=(2l+1)^{1/2}$ and the C coefficients are given by

$$C(n_1'l_1'n_2l_2; n_1l_1n_2'l_2'; L, p) = \sum_{N\mathfrak{L}nn'l} B(nln'l; p)\langle nlN\mathfrak{L}, L \mid n_1'l_1'n_2l_2, L\rangle\langle n'lN\mathfrak{L}, L \mid n_1l_1n_2'l_2', L\rangle. \quad (6)$$

The transformation brackets $\langle nlN\mathfrak{L}, L \mid n_1l_1n_2l_2, L\rangle$ and B coefficients are defined and tabulated by Brody and Moshinsky.[21] Talmi integrals are given by

$$I_p(V)=\frac{2}{\Gamma(p+\frac{3}{2})}\int_0^\infty x^{2p+2}e^{-x^2}V(b'x)\,dx, \quad (7)$$

where $b'=\sqrt{2}b=(2/M\omega_0)^{1/2}$, ω_0 is the oscillator energy, and M is the nucleon mass. Following LW, the potential $v(1, 2)$ was taken to be a Serber-Yukawa force with parameters adjusted to fit low-energy n-p scattering data[7]

$$\begin{aligned} v(1,2) &= [{}^1v(r_{12}){}^1P + {}^3v(r_{12}){}^3P][\tfrac{1}{2}(1+P_M(1,2))], \\ {}^1P &= \tfrac{1}{4}(1-\boldsymbol{\sigma}_1\cdot\boldsymbol{\sigma}_2), \qquad {}^3P=\tfrac{1}{4}(3+\boldsymbol{\sigma}_1\cdot\boldsymbol{\sigma}_2), \\ v(r_{12}) &= V_0[\exp(-\mu r_{12})/\mu r_{12}], \qquad {}^1V_0=-46.87 \text{ MeV}, \quad {}^1\mu=0.8547 \text{ F}^{-1} \\ & \qquad\qquad {}^3V_0=-52.13 \text{ MeV}, \quad {}^3\mu=0.7261 \text{ F}^{-1} \end{aligned} \quad (8)$$

where $P_M(1, 2)$ is the Majorana exchange operator. In the case of a Serber force, the sum over l in the definition of the C coefficients reduces to a sum over even values of l only.

Once the secular matrix has been diagonalized and the coefficients $\alpha_{JT}{}^{K}$ have been obtained, the matrix elements of the required multipole operators $\mathfrak{M}_{JT}$ are given by

$$|(\Psi_{JT}\vdots\vdots\mathfrak{M}_{JT}\vdots\vdots\Psi_0)|^2 = \Big|\sum_{n_1l_1j_1,n_2l_2j_2} \alpha_{JT}{}^{(n_1l_1j_1)(n_2l_2j_2)-1} \times (n_1l_1j_1\vdots\vdots\mathfrak{M}_{JT}\vdots\vdots n_2l_2j_2)\Big|^2, \quad (9)$$

where the symbols $\vdots\vdots$ are used for matrix elements reduced in both angular momentum and isospin. The problem is then one of finding single-particle matrix elements of the multipole operators.

The inelastic-electron-scattering cross section in first Born approximation may be written[2]

$$d\sigma/d\Omega = 4\pi\sigma_M(E_0,\theta)/[1+(2E_0\sin^2(\tfrac{1}{2}\theta))/M_T] \times\{(q_\mu^2/q^2)^2F_L^2(q)+[(q_\mu^2/2q^2)+\tan^2(\tfrac{1}{2}\theta)]F_T^2(q)\}, \quad (10)$$

where E_0 is the incident electron energy, θ is the angle the electron is scattered through, M_T is the target mass, $q_\mu=(\mathbf{q},i\omega)$ is the four-momentum transfer, $q=|\mathbf{q}|$ is the magnitude of the three-momentum transfer, and $\sigma_M(E_0,\theta)$ is the Mott cross section

$$\sigma_M(E_0,\theta)=[\alpha\cos(\tfrac{1}{2}\theta)/2E_0\sin^2(\tfrac{1}{2}\theta)]^2. \quad (11)$$

$F_L^2(q)$ and $F_T^2(q)$ are the longitudinal and transverse inelastic form factors, respectively, and for a spin-0

[21] T. A. Brody and M. Moshinsky, *Tables of Transformation Brackets* (Universidad Nacional Autonoma de Mexico, Mexico, 1960).

target nucleus are given by

$$F_L^2(q)=\tfrac{1}{3}f_{SN}^2(q_\mu^2)\,g_{\text{c.m.}}^2(q^2)\sum_{J=0}^{\infty}|\,(\Psi_{JT}\vdots\vdots\hat{M}_{JT}^{\text{Coul}}(q)\vdots\vdots\Psi_0)\,|_{T=1}^2, \tag{12}$$

$$F_T^2(q)=F_{\text{el}}^2(q)+F_{\text{mag}}^2(q)=\tfrac{1}{3}f_{SN}^2(q_\mu^2)\,g_{\text{c.m.}}^2(q^2)$$
$$\times\sum_{J=1}^{\infty}\{|\,(\Psi_{JT}\vdots\vdots\hat{T}_{JT}^{\text{el}}(q)\vdots\vdots\Psi_0)\,|^2+|\,(\Psi_{JT}\vdots\vdots\hat{T}_{JT}^{\text{mag}}(q)\vdots\vdots\Psi_0)\,|^2\}_{T=1}, \tag{13}$$

where $F_{\text{el}}^2(q)$ and $F_{\text{mag}}^2(q)$ are the electric and magnetic form factors, respectively. In first Born approximation, the finite size of the nucleon is incorporated by multiplying by the single-nucleon form factor, taken here to be[1]

$$f_{SN}(q_\mu^2)=(1+q_\mu^2/q_N^2)^{-2},\qquad q_N=855\ \text{MeV}/c. \tag{14}$$

Finally, the c.m. correction $g_{\text{c.m.}}(q^2)$ is included. This takes the form[2,22,23]

$$g_{\text{c.m.}}(q^2)=e^{y/A},\qquad y=(bq/2)^2 \tag{15}$$

for harmonic-oscillator wave functions.

In considering single-particle-hole states, we require reduced matrix elements of the multipole operators[2]

$$\hat{M}_{JM}^{\text{Coul}}(q)=[e_i+(q_\mu^2/8M^2)\,(e_i-2\mu_i)\,]M_J^M(\mathbf{r}_i), \tag{16}$$

where the term involving $(q/M)^2$ is the Darwin-Foldy correction.[2,24]

$$\hat{T}_{JM}^{\text{el}}(q)=\frac{q}{M}\left\{e_i\left(-\frac{(J)^{1/2}}{[J]}\mathbf{M}_{JJ+1}^M(\mathbf{r}_i)+\frac{(J+1)^{1/2}}{[J]}\mathbf{M}_{JJ-1}^M(\mathbf{r}_i)\right)\cdot q^{-1}\boldsymbol{\nabla}+\tfrac{1}{2}\mu_i\mathbf{M}_{JJ}^M(\mathbf{r}_i)\cdot\boldsymbol{\sigma}(i)\right\}, \tag{17}$$

$$i\hat{T}_{JM}^{\text{mag}}(q)=\frac{q}{M}\left\{\tfrac{1}{2}\mu_i\left(\frac{(J)^{1/2}}{[J]}\mathbf{M}_{JJ+1}^M(\mathbf{r}_i)-\frac{(J+1)^{1/2}}{[J]}\mathbf{M}_{JJ-1}^M(\mathbf{r}_i)\right)\cdot\boldsymbol{\sigma}(i)+e_i\mathbf{M}_{JJ}^M(\mathbf{r}_i)\cdot q^{-1}\boldsymbol{\nabla}\right\}, \tag{18}$$

where

$$\begin{aligned}M_J^M(\mathbf{x})&=j_J(qx)\,Y_J^M(\Omega_x),\\ \mathbf{M}_{JL}^M(\mathbf{x})&=j_L(qx)\,\mathbf{Y}_{JL1}^M(\Omega_x),\end{aligned} \tag{19}$$

and

$$\begin{aligned}e_i&=\tfrac{1}{2}(1+\tau_3(i)),\\ \mu_i&=\tfrac{1}{2}(\mu_S+\mu_V\tau_3(i)).\end{aligned} \tag{20}$$

The necessary reduced matrix elements are given by

$$(n_1(l_1\tfrac{1}{2})j_1\,||\,M_J(\mathbf{r})\,||\,n_2(l_2\tfrac{1}{2})j_2)=(-)^{J+j_2+1/2}(4\pi)^{-1/2}[l_1][l_2][j_1][j_2][J]$$
$$\times\begin{Bmatrix}l_1 & j_1 & \frac{1}{2}\\ j_2 & l_2 & J\end{Bmatrix}\begin{pmatrix}l_1 & J & l_2\\ 0 & 0 & 0\end{pmatrix}(n_1l_1\,|\,j_J(\rho)\,|\,n_2l_2), \tag{21}$$

$$(n_1(l_1\tfrac{1}{2})j_1\,||\,\mathbf{M}_{JL}(\mathbf{r})\cdot\boldsymbol{\sigma}\,||\,n_2(l_2\tfrac{1}{2})j_2)=(-)^{l_1}(6/4\pi)^{1/2}[l_1][l_2][j_1][j_2][L][J]$$
$$\times\begin{Bmatrix}l_1 & l_2 & L\\ \frac{1}{2} & \frac{1}{2} & 1\\ j_1 & j_2 & J\end{Bmatrix}\begin{pmatrix}l_1 & L & l_2\\ 0 & 0 & 0\end{pmatrix}(n_1l_1\,|\,j_L(\rho)\,|\,n_2l_2), \tag{22}$$

$$(n_1(l_1\tfrac{1}{2})j_1\,||\,\mathbf{M}_{JL}(\mathbf{r})\cdot q^{-1}\boldsymbol{\nabla}\,||\,n_2(l_2\tfrac{1}{2})j_2)=(-)^{L+j_2+1/2}(4\pi)^{-1/2}[l_1][l_2][j_1][j_2][L][J]$$
$$\times\begin{Bmatrix}l_1 & j_1 & \frac{1}{2}\\ j_2 & l_2 & J\end{Bmatrix}\Bigg[-(l_2+1)^{1/2}[l_2+1]/[l_2]\begin{Bmatrix}L & 1 & J\\ l_2 & 1 & l_2+1\end{Bmatrix}\begin{pmatrix}l_1 & L & l_2+1\\ 0 & 0 & 0\end{pmatrix}$$
$$\times(n_1l_1\,|\,j_L(\rho)\left(\frac{d}{d\rho}-\frac{l_2}{\rho}\right)|\,n_2l_2)+(l_2)^{1/2}[l_2-1]/[l_2]$$
$$\times\begin{Bmatrix}L & 1 & J\\ l_2 & 1 & l_2-1\end{Bmatrix}\begin{pmatrix}l_1 & L & l_2-1\\ 0 & 0 & 0\end{pmatrix}(n_1l_1\,|\,j_L(\rho)\left(\frac{d}{d\rho}+\frac{l_2+1}{\rho}\right)|\,n_2l_2)\Bigg], \tag{23}$$

[22] J. P. Elliott and T. H. R. Skyrme, Proc. Roy. Soc. (London) **A232**, 561 (1955).
[23] S. Gartenhaus and C. Schwartz, Phys. Rev. **108**, 482 (1957).
[24] K. W. McVoy and L. VanHove, Phys. Rev. **125**, 1034 (1962).

where $\rho=qr$ and where the radial matrix elements involving derivatives can be reduced to matrix elements of spherical Bessel functions only, the latter being given by

$$(n'l' \mid j_L(qr) \mid nl)=\frac{2^L}{(2L+1)!!}y^{L/2}e^{-y}[(n'-1)!(n-1)!$$
$$\times\Gamma(n'+l'+\tfrac{1}{2})\Gamma(n+l+\tfrac{1}{2})]^{1/2}\sum_{m'=0}^{n'-1}\sum_{m=0}^{n-1}\frac{(-)^{m'+m}}{m'!m!(n'-m'-1)!(n-m-1)!}$$
$$\times\frac{\Gamma(\frac{1}{2}(l'+l+2m'+2m+L+3))}{\Gamma(l'+m'+\frac{3}{2})\Gamma(l+m+\frac{3}{2})}F(\tfrac{1}{2}(L-l'-l-2m'-2m);L+\tfrac{3}{2};y). \quad (24)$$

For all cases here, the confluent hypergeometric function $F(\alpha;\beta;y)$ reduces to a simple polynomial in y. Explicit expressions for reduced matrix elements of the multipole operators required here are tabulated in the Appendix.

III. RESULTS

The single-particle energies and consequently the unperturbed energies of the particle-hole states considered here are[6]

$$\epsilon_{1s_{1/2}}=35 \text{ MeV}, \quad \epsilon_{1p_{3/2}}=18.72 \text{ MeV},$$
$$\epsilon_{1p_{1/2}}=4.95 \text{ MeV},$$
$$\epsilon_{2s_{1/2}}=1.86 \text{ MeV}, \quad \epsilon_{1d_{5/2}}=1.10 \text{ MeV},$$
$$\epsilon_{1d_{3/2}}=-3.39 \text{ MeV},$$
$$E_0(1p_{1/2})(1p_{3/2})^{-1}{}_{1^+,2^+}=13.77 \text{ MeV},$$
$$E_0(2s_{1/2})(1p_{3/2})^{-1}{}_{1^-,2^-}=16.86 \text{ MeV},$$
$$E_0(1d_{5/2})(1p_{3/2})^{-1}{}_{1^-,2^-,3^-,4^-}=17.62 \text{ MeV},$$
$$E_0(1d_{3/2})(1p_{3/2})^{-1}{}_{0^-,1^-,2^-,3^-}=22.11 \text{ MeV},$$
$$E_0(1p_{1/2})(1s_{1/2})^{-1}{}_{0^-,1^-}=30.05 \text{ MeV}.$$

The pure particle-hole states are shifted from their unperturbed energies when a residual interaction is introduced. The level scheme for the pure states (no configuration mixing) is shown in Fig. 1 as a function of the oscillator parameter b, where the Serber-Yukawa force of Eq. (8) has been used.[25] When configuration mixing is allowed and the Hamiltonian is diagonalized to yield energy eigenvalues and eigenvectors, we obtain the level scheme shown in Fig. 2. The calculation here is the same as that of LW and deForest,[26] extended to 1^+, 2^+, 3^-, and 4^- states and to a range of values of the oscillator parameter. In subsequently discussing the electron scattering results, the oscillator parameter will be fixed at $b=1.64$ F to yield agreement for the C^{12} elastic form factor[27] and to compare favorably with the value obtained from Coulomb energy differences, $b=1.66$ F.[28] In I, the value 1.60 F was used; however, the results obtained with either value are very similar. The states obtained are listed in Table I.

Experimentally a 1^+ level is found at 15.1 MeV and 2^+ level at 16.1 MeV, whereas with the residual interaction considered here this doublet is inverted and lies too high. Vinh-Mau and Brown[29] obtain a 1^+ at 16.1 MeV and a 2^+ at 16.5 MeV, both corresponding to almost pure configurations. In their calculation, a different spin dependence was used in the residual interaction resulting in closer agreement with the experimental energy values. In more detailed intermediate-coupling calculations[30] one finds more mixing of configurations, however, the dominant effect is simply to lower the over-all transition strength to these levels and leave the momentum dependence relatively unchanged.

The next observed level is a 2^- at 16.6 MeV. We identify this with the lowest 2^- we have, that is the one dominated by the $(1p_{3/2})^{-1}(2s_{1/2})$ pure particle-hole state. In considering electron scattering data averaged over energy intervals on the order of 1 MeV as we are doing here, the 2^+ at 16.1 MeV and the 2^- at 16.6 MeV are taken together to form the 16-MeV complex. The form factors for this complex will be considered later.

Next we identify our lowest 1^- level [dominated by the $(1p_{3/2})^{-1}(2s_{1/2})$ pure particle-hole state] with the feature found at 18.1 MeV in electron scattering at low momentum transfer. Both our 1^- and 2^- states dominated by $(1p_{3/2})^{-1}(2s_{1/2})$ are found to lie too high. If they are identified with the lower-lying experimental states as we have done, there remain 2^-, 3^-, and 4^- levels in the 19–20-MeV region, all dominated by the $(1p_{3/2})^{-1}(1d_{5/2})$ pure state (in fact, this is the only way to get a single-particle-hole 4^- state with the shells considered here). This collection of states we will call the 19-MeV complex and will consider as a unit when electron scattering form factors are examined. The 2^- is believed to be the giant magnetic quadrupole resonance in C^{12}.[26] Vinh-Mau and Brown's calculation places this level at 19.2 MeV. The 3^- level has been seen[31] at 18.6 MeV and has previously been discussed both on the basis of a harmonic-oscillator shell model

[25] Note that in I the energies were given for b in the range 1.9–2.2 F rather than 1.6–1.9 F as stated.
[26] T. deForest, Jr., Phys. Rev. **139**, B1217 (1965).
[27] T. W. Donnelly and G. E. Walker, Phys. Rev. Letters **22**, 1121 (1969).
[28] G. E. Walker (private communication).
[29] N. Vinh-Mau and G. E. Brown, Nucl. Phys. **29**, 89 (1962).
[30] D. Kurath, Phys. Rev. **134**, B1025 (1964).
[31] W. Feldman, M. Suffert, and S. S. Hanna, Bull Am. Phys. Soc. **13**, 822 (1968).

TABLE I. Energies and wave functions for J^-, $T=1$ states with $b=1.64$ F.

J	E (MeV)	$(2s_{1/2})(1p_{3/2})^{-1}$	$(1d_{5/2})(1p_{3/2})^{-1}$	$(1d_{3/2})(1p_{3/2})^{-1}$	$(1p_{1/2})(1s_{1/2})^{-1}$
0	25.53			0.936	−0.352
	35.45			0.352	0.936
1	19.52	0.978	−0.165	0.129	−0.016
	23.09	0.188	0.958	−0.192	0.095
	24.89	−0.089	0.229	0.940	−0.238
	35.55	−0.025	−0.040	0.252	0.967
2	18.80	0.939	−0.344	−0.024	
	20.60	0.337	0.931	−0.140	
	23.83	0.070	0.124	0.990	
3	19.24		0.992	0.123	
	25.09		−0.123	0.992	
4	20.17		1.000		

and of a continuum model with configuration mixing by Friar,[32] who found, as we also find here, that this state is composed almost entirely of the $(1p_{3/2})^{-1}(1d_{5/2})$ pure configuration. No independent evidence exists for the 4^- state, which is found here to lie within several hundred keV of the 2^- state.

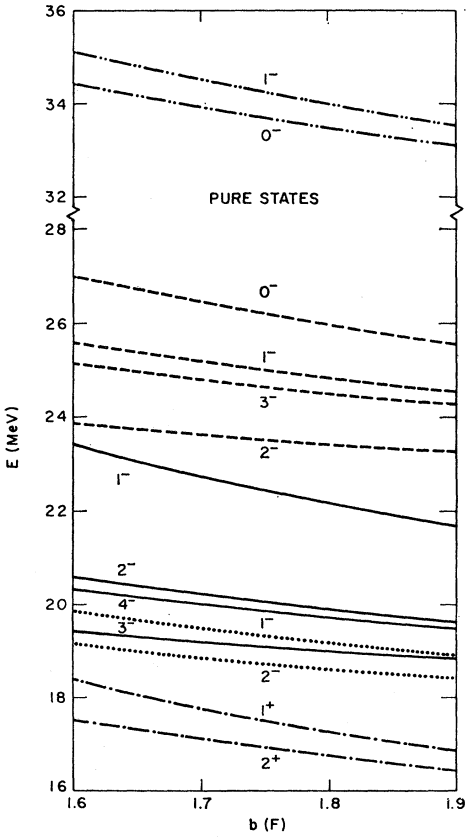

FIG. 1. The energy eigenvalues of the pure particle-hole states as a function of the oscillator parameter b for a Serber-Yukawa residual interaction.

[32] J. Friar, thesis, Stanford University, 1967 (unpublished).

In considering the states dominated by the $(1p_{3/2})^{-1}(1d_{3/2})$ pure particle-hole state, we find a 3^- around 25 MeV and a 0^- about $\frac{1}{2}$ MeV higher. The 0^- is not excited by electrons. Friar[32] has shown that in a continuum calculation the 3^- lies at about 27 MeV. Consequently, we consider only the remaining levels in the 21–25-MeV region, the 1^- dominated by the

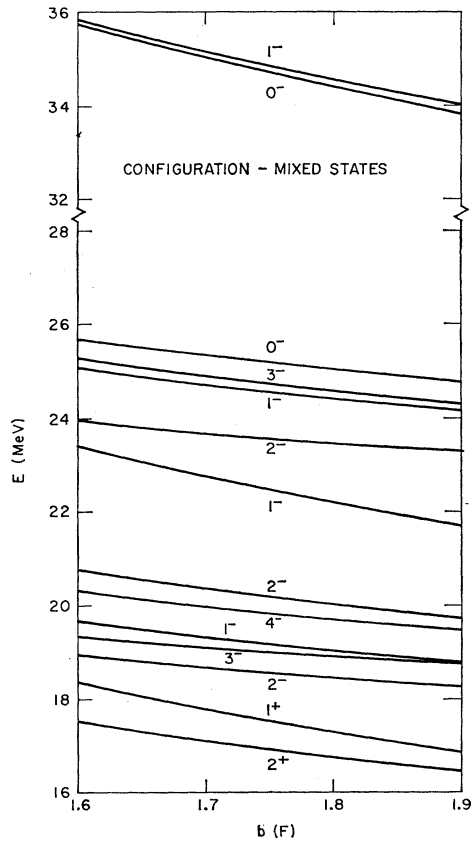

FIG. 2. The energy eigenvalues of the configuration-mixed particle-hole states as a function of the oscillator parameter b for a Serber-Yukawa residual interaction.

$(1p_{3/2})^{-1}(1d_{5/2})$ and the 1^- and 2^- dominated by the $(1p_{3/2})^{-1}(1d_{3/2})$, and identify them taken together as a complex with the giant resonance centered at 22.8 MeV in photoexcitation.

Altogether, there are these five gross features in the range 15–25 MeV: a 1^+ at 15.1 MeV, a 16-MeV complex, a 1^- at 18.1 MeV, a 19-MeV complex, and a giant resonance at about 23 MeV. The electron scattering data for C^{12} in this energy range, in fact, have these features as gross structure and no others. At low momentum transfer where the resolution in recent experiments[3] is highest, these complexes are seen to have fine structure, but with our policy of comparing only the averaged data to calculations including just the 1p–1h excitations, we do not attempt to make a more detailed decomposition of the complexes.

To obtain the electron scattering form factors, the reduced matrix elements of the appropriate multipole operators are required. Expressions for these matrix elements for the pure particle-hole states considered here are tabulated in the Appendix. The form factors for the configuration-mixed states are then obtained in Eq. (9) as linear combinations of the pure state form factors with mixing coefficients given in Table I. Finally, the complexes are incoherent combinations of the configuration-mixed form factors.

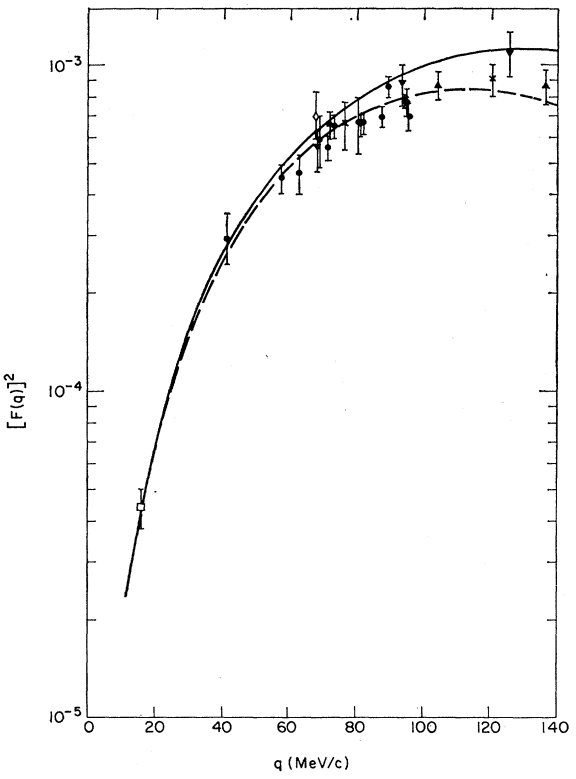

FIG. 3. The $M1$ form factor for the 15.1-MeV 1^+ level. The solid curve is for an oscillator parameter of 1.64 F and the dashed curve for 1.9 F. The calculated amplitude has been divided by 2. The data shown are ○ Ref. 8, × Ref. 9, ▲ Ref. 10, ◇ Ref. 11, ● Ref. 12, □ Ref. 13, and ▼ Ref. 20.

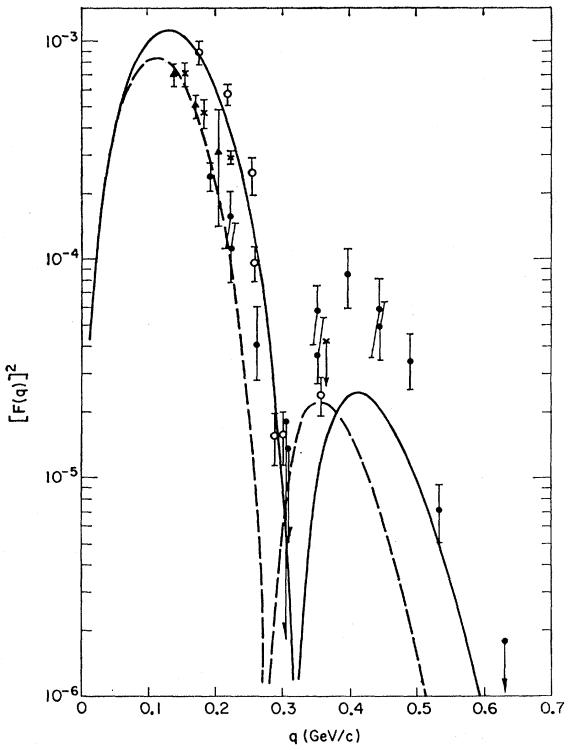

FIG. 4. $M1$ form factor as for Fig. 3. The solid curve is for $b=1.64$ F and the dashed curve for $b=1.9$ F. The data given are ●Ref. 3, ○ Ref. 8, × Ref. 9, and ▲ Ref. 10.

The 1^+, $M1$ form factor is shown in Figs. 3 and 4. The quantity plotted in all the figures and called the form factor is

$$F^2(q)=F_L^2(q)/[\tfrac{1}{2}+\tan^2(\tfrac{1}{2}\theta)]+F_T^2(q) \qquad (25)$$

with all the angle dependence contained in the longitudinal contribution. Of course for wrong parity (magnetic) transitions such as this $M1$ form factor there is no longitudinal contribution at all. Two values of the oscillator parameter are considered: $b=1.64$ F to agree with the elastic form-factor determination and $b=1.9$ F to agree with a previous fit[12] to the low-momentum-transfer data (Fig. 3). The amplitude (reduced matrix element) has been reduced by a factor 2 to agree with the low-q data, indicating that the single-particle-hole picture of this excitation cannot be correct in detail, even though it can produce the correct momentum-transfer dependence.[30] Particularly noteworthy is the prediction of a diffraction minimum in the form factor, in qualitative agreement with the recent data of Sick and Hughes.[3] This is believed to be the first clear published evidence for a diffraction minimum in an inelastic-electron-scattering form factor.

In Fig. 5, the form factor for the 16-MeV complex is shown. The 2^+, $C2+E2$ form factor has been reduced in amplitude by the same factor of 2 as the 1^+ (these states differ only in the coupling of angular momenta to $J=1$ or 2). The longitudinal form factors presented here are divided by $\frac{1}{2}+\tan^2(\frac{1}{2}\theta)$ (which equals 6.33 for

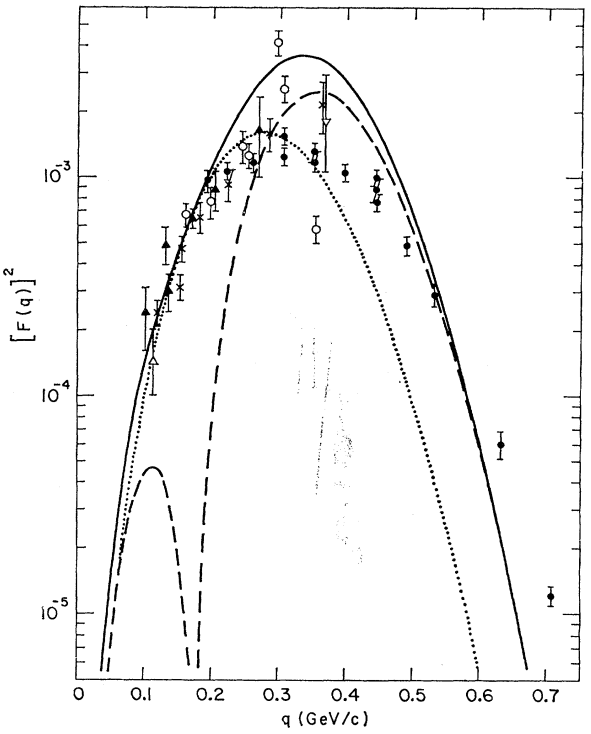

FIG. 5. The 16-MeV complex form factor at $\theta=135°$. The dotted curve is the 2^+, $C2+E2$ form factor (with amplitude reduced by a factor of 2). The dashed curve is the $M2$ form factor for the 2^- state at 18.80 MeV in the present calculation. The solid curve is the sum. The data shown are ● Ref. 3, ○ Ref. 8, × Ref. 9, ▲ Ref. 10, ▽ Ref. 14, and △ Ref. 15. Note that the data of Ref. 8 are for the 2^+ level only.

$\theta=135°$), whereas the transverse form factors have no angle dependence. For the 2^+ state the $C2$ contribution (i.e., divided by 6.33) is larger than the $E2$ contribution at small momentum transfer, the two are equal at about 130 MeV/c, and at higher q the $E2$ dominates. Figure 5 shows the sum of the $C2$ and $E2$ contributions. The predicted general behavior of the 16-MeV complex as a function of momentum transfer is in agreement with experiment, although it could be improved in the region $q\sim$200–500 MeV/c by reducing the 2^-, $M2$ amplitude somewhat. At high q the 2^- form factor is dominant and, in particular, the $(1p_{3/2})^{-1}(2s_{1/2})$ part of the 2^- state is what determines the amplitude there, being much larger than the $(1p_{3/2})^{-1}(1d_{5/2})$ or $(1p_{3/2})^{-1}(1d_{3/2})$ contributions. By examining the q dependence of the form factors in this way information can be obtained about the configurations which constitute the wave function. The calculated form factors for the 16-MeV complex (and indeed for all the form factors considered here) decrease too rapidly with increasing momentum transfer beyond about 500 MeV/c. Similar results are obtained for the elastic form factor[27] and to some extent may be changed by using finite-well wave functions rather than the Gaussian-like harmonic-oscillator wave functions that are used here.

The form factor for the 1^-, $C1+E1$ excitation identified with the state at 18.1 MeV is shown in Fig. 6. The data extend only to $q\sim$300 MeV/c, beyond which the tail of the larger 19-MeV complex dominates. The $E1$ is larger than the $C1$ contribution for all q except near 300 MeV/c, where the $E1$ has a diffraction zero; indeed the $E1$ is finite at $q=0$ whereas the $C1$ form factor is proportional to q at small q.

The 19-MeV complex form factor is shown in Fig. 7. From the q dependence at small momentum transfer the existence of the 2^-, $M2$ excitation can be inferred.[26] However, the 2^- form factor has a diffraction minimum at about 330 MeV/c, where the data have none. If, instead of the particle-hole model, the Goldhaber–Teller model is used for the giant magnetic quadrupole resonance,[33] the 2^- form factor still has a diffraction minimum, in this case at the elastic form-factor value of about 360 MeV/c. Indeed the form factors obtained on the basis of these two models are very similar. The 3^-, $C3+E3$ excitation shown in Fig. 8 is predominantly longitudinal and small and so cannot fill in the 2^- diffraction minimum. Alternatively, including the 1^- which was identified with the feature at 18.1 MeV gives the wrong q dependence at low momentum transfer. There remains the 4^-, $M4$ excitation to consider among the levels found in this energy region

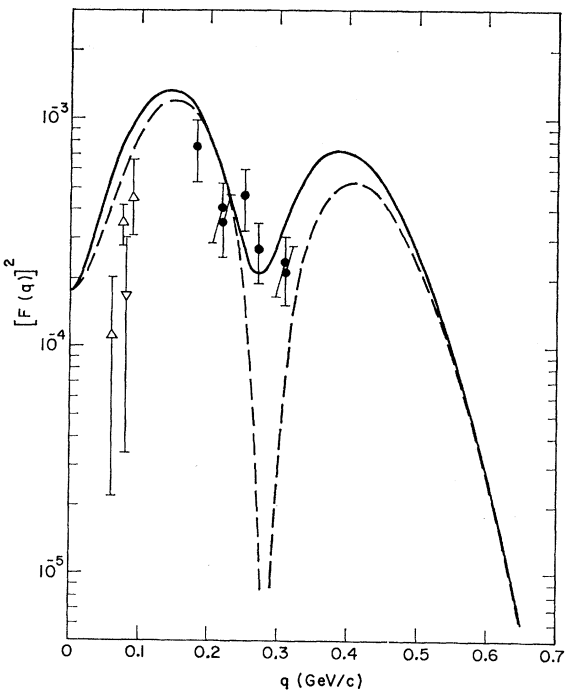

FIG. 6. The $C1+E1$ form factor for the 1^- state at 19.52 MeV. The dashed curve is the $E1$ only; the solid curve is the sum of the $E1$ and $C1$ for $\theta=135°$. The data are for the feature observed at 18.1 MeV: ● Ref. 3, ▽ Ref. 17 ($\theta=128°$), and △ Ref. 17 ($\theta=152°$).

[33] H. Uberall, Nuovo Cimento **41B**, 25 (1966).

(Fig. 2). As seen in Fig. 7, when the 2^-, 3^-, and 4^- are taken together the calculated and experimental form factors are in reasonable agreement. This agreement could again be improved by reducing the calculated amplitude by a factor of about $\sqrt{2}$.[26,34] In Fig. 8, experimental upper limits on the longitudinal contribution to the 19-MeV complex are shown and compared with the 3^- form factor. The large-momentum-transfer dependence of the 2^- form factor is again due mainly to the $(1p_{3/2})^{-1}(2s_{1/2})$ configuration even though there is more of the $(1p_{3/2})^{-1}(1d_{5/2})$ present in the configuration-mixed wave function (cf. Table I). On the other hand, the 4^- form factor results from a pure $(1p_{3/2})^{-1}(1d_{5/2})$ particle-hole state and obtains its large amplitude at high momentum transfer from the high power of q in the expression for the form factor (q^4 in the matrix element or q^8 in the cross section, cf. the Appendix). Of course, because of this high power of q, the $M4$ is very small at small momentum transfer and consequently very difficult to observe except in a process such as electron scattering (far off the photon mass shell). Except for

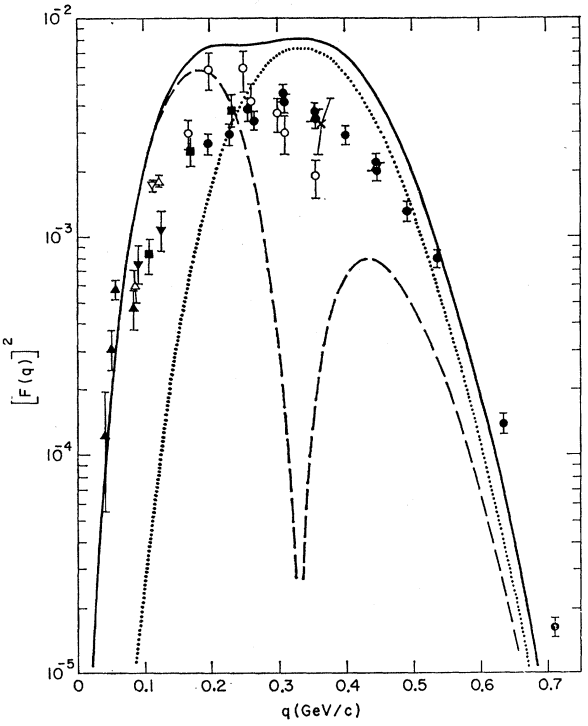

FIG. 7. The 19-MeV complex form factor at $\theta=135°$. The dashed curve is the $M2$ form factor of the 20.60-MeV 2^- level and the dotted curve is the $M4$ form factor of the 20.17-MeV 4^- level. The sum of the 2^-, 3^- at 19.24-MeV ($C3+E3$) and 4^- form factors is given as the solid curve. The data presented are ● Ref. 3, ○ Ref. 8, × Ref. 14, ▽ and △ Ref. 15, ■ Ref. 16, ▲ and ▼ Ref. 17. Note that the 4^- form factor given in I was plotted too low.

[34] Previous work (Ref. 26) has shown that the calculated 2^- giant quadrupole form factor is too large in amplitude by a actor of about $\sqrt{2}$.

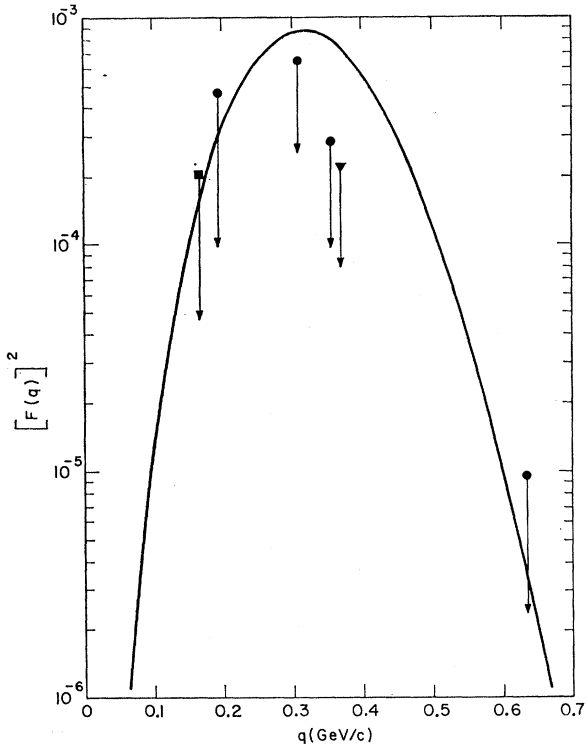

FIG. 8. The 19.24-MeV $C3$ form factor at $\theta=135°$ {i.e., $F_L^2(q)/[\frac{1}{2}+\tan^2(\frac{1}{2}\theta)]$}. The experimental upper limits on this longitudinal contribution are ● Ref. 3, ▼ Ref. 14, and ■ Ref. 16.

the "fall off" at high q, the agreement for both longitudinal and transverse form factors with experiment is good. In Fig. 9, the 19-MeV complex is shown with the 40° data of Crannell *et al.*[18] At this smaller angle the longitudinal form factor plays a much more important role.

The treatment of the giant resonance region is complicated by the continuum quasielastic background which, particularly at high momentum transfer where the giant resonance is small, makes a separation of resonant and nonresonant contributions difficult. In I, we took two limiting approximations: first, that the quasielastic contribution was linear with energy beginning at the neutron threshold of 18.7 MeV and matching the data at 27–32 MeV, i.e., at energies above the giant resonance (see Figs. 10 and 11), and second, that there was no quasielastic contribution at all. The proton threshold is, in fact, at 16.0 MeV, however, with a Coulomb barrier for protons it is probably reasonable to take the neutron threshold for both kinds of nucleons. The results obtained in I consequently showed a large spread between the two ways of considering the quasielastic background. In the present work, a somewhat better approach is taken. The nonresonant background contribution is obtained by summing all non-negligible multipole transitions to pure particle-hole states (no residual interaction)

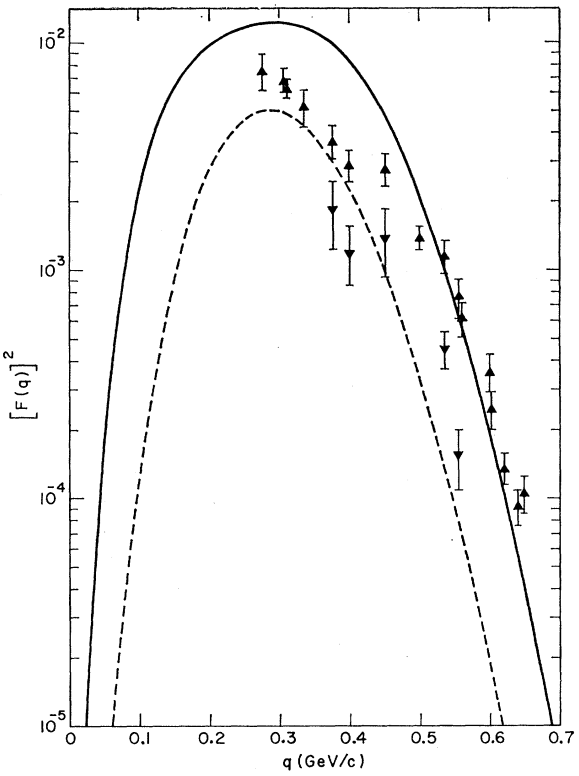

FIG. 9. The 19-MeV complex form factor at $\theta=40°$. The solid curve is the $2^-+3^-+4^-$ total form factor and the dashed curve the longitudinal ($C3$) contribution only. The data are from Ref. 18.

using square-well wave functions. From an examination of the elastic form factor with finite-well wave functions, reasonable parameters can be chosen for the square well: a radius of $R=3.0$ F and a well depth of $V=48.7$ MeV to give the $1p$ single-particle state the neutron separation energy $E_{1p}=18.7$ MeV. The $1s$ single-particle energy in this well is $E_{1s}=33.7$ MeV.

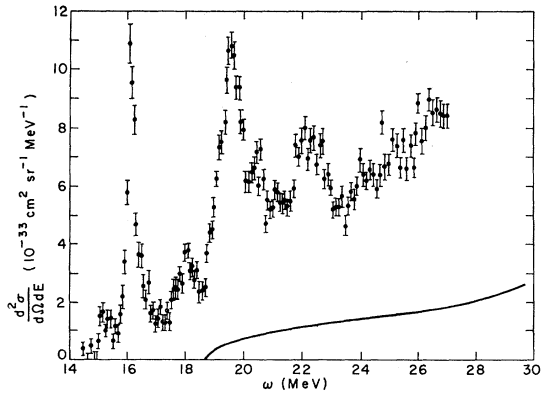

FIG. 10. The inelastic cross section for $\theta=135°$ and an incident electron energy $E_0=131$ MeV. The data are from Ref. 3 with radiative effects removed. The solid curve is the calculated quasielastic contribution to the cross section.

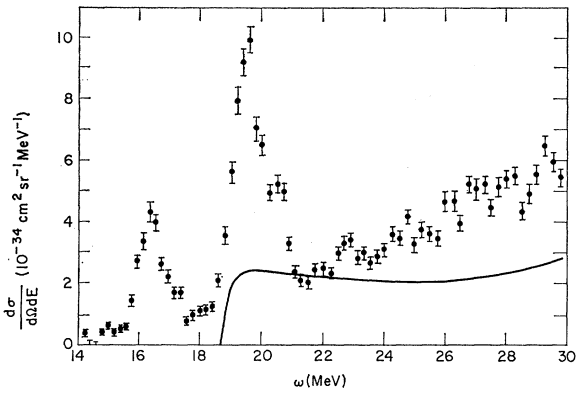

FIG. 11. As for Fig. 10, except at $\theta=135°$ and $E_0=275$ MeV. Note that the form factor for the 19-MeV complex given in Ref. 3 may be slightly too large due to the smaller quasielastic background assumed there than calculated in the present work.

Using these $1s$ and $1p$ wave functions the elastic form factor for C^{12} was calculated and compared with experiment[27]; in fact, the radius parameter R was chosen from among several that were tried by requiring that the calculated elastic form factor have its first diffraction minimum at the experimental value. In this square-well potential with no spin-orbit splitting, the $1d$ state is bound by 1.38 MeV compared to the single-particle energies of the $1d_{5/2}$ state (1.10 MeV, bound) and the $1d_{3/2}$ state (−3.39 MeV, unbound)

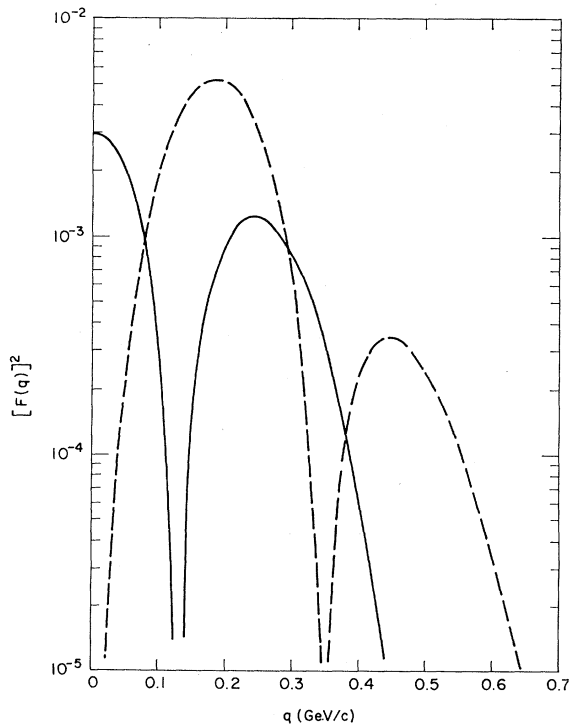

FIG. 12. The $E1$ form factors for the 1^- states at 23.09 MeV (solid curve) and 24.89 MeV (dashed curve).

which are used in the rest of this work. With the $1d$ state below threshold and no mixing of bound and continuum states the main strength is to the same particle-hole states considered above using a harmonic-oscillator basis. There will also be a contribution for excitation energies above threshold from particle-hole states having bound (hole) and continuum (particle) wave functions which is generally called the quasielastic contribution. To obtain this quasielastic cross section all significant multipole transitions to single-particle (continuum)–single-hole states are summed. Both bound and continuum wave functions are computed in the same square-well potential. The results are shown in Figs. 10 and 11 and compared with the data of Sick and Hughes.[3] An important observation here is that at low q (Fig. 10) the quasielastic contribution is relatively small and the giant resonance dominates the excitation function in the region $\omega=21$–27 MeV; on the other hand, at high q (Fig. 11) the quasielastic contribution is relatively large and the giant resonance has nearly disappeared. The rapid rise from threshold of the cross section is principally due to multipole transitions which involve s waves in the continuum. However, higher partial waves are, in general, important and indeed for values of momentum transfer around 200 MeV/c the p and d waves contribute more than the s waves do at excitation energies as low as several hundred keV above threshold. In this calculation, the protons have been treated like neutrons in that the neutron separation energy is used and the Coulomb barrier is ignored. If the correct separation energy of 16.0 MeV is used for protons, then the cross section will begin at that value as well. However, the presence of the Coulomb barrier will decrease the cross section near threshold and will likely yield results similar to those obtained here by treating protons and neutrons alike. This may not be true in some particular range of momentum transfer where an enhancement similar to that obtained here for higher partial waves may occur, but it is likely true for most values of q.

Using this estimate of the quasielastic contribution, we proceed to a consideration of the giant resonance region. The quasielastic form factor which results when the calculated double-differential cross section is integrated between $\omega=21$ MeV and $\omega=27$ MeV (the same range as used for the data of Sick and Hughes[3] and the data of Ricco *et al.*[19]) is shown in Fig. 13 (dotted curve). The main contribution in the neighborhood of $q=200$ MeV/c is $E1$, followed in importance by $M2$ and $M1$ multipoles. On the other hand at $q\sim400$ MeV/c the most important term is $M2$, followed by $E1$, $E3$, $M3$, and $E2$, respectively. The cross sections presented here, in fact, have all multipoles up to at least $C6$, $E6$, and $M7$ included, although the higher multipoles are extremely small. At low q, the Coulomb cross section is larger than the transverse cross section, but the two become comparable when the $\frac{1}{2}+\tan^2(\frac{1}{2}\theta)$ factor is included as this enhances the transverse contribution by 6.33 for $\theta=135°$. At high q the longitudinal and transverse form factors are comparable in magnitude and with the factor 6.33 the transverse cross section is consequently dominant.

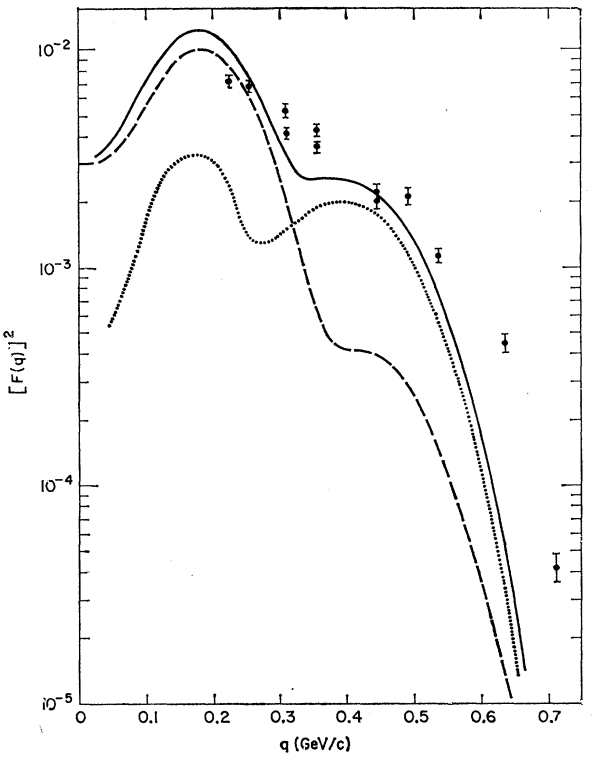

FIG. 13. The giant-resonance-region form factor at $\theta=135°$. The dashed curve is the sum of the form factors for the 1^- levels at 23.09 and 24.89 MeV and the 2^- level at 23.83 MeV. Following the argument in Ref. 6 the $C1$ form factors have been divided by 2. The dotted curve is the calculated quasielastic form factor for cross sections integrated between $\omega=21$ MeV and $\omega=27$ MeV. The solid curve is the sum. The data from Ref. 3 are also for cross sections integrated in energy between 21 and 27 MeV.

To determine the importance of using continuum wave functions which are solutions to the Schrödinger equation in the presence of a nuclear square-well potential, the same calculation was repeated using plane waves ($V=0$) for the particle wave functions. The bound-state solutions in the square well were retained for the hole wave functions. The Coulomb form factor, for example, then involves essentially the Fourier transform of the ground-state charge distribution. The results differ appreciably: At low momentum transfer the plane wave case yields form factors which are larger than in the case of distorted waves (for example, 3 times larger at $q=200$ MeV/c). For high q the reverse is true—the form factor for $V=48.7$ MeV is larger than the form factor for $V=0$ (for example, by a factor of 9 at $q=400$ MeV/c). The result is that including the nuclear potential for the continuum wave functions is indeed important.

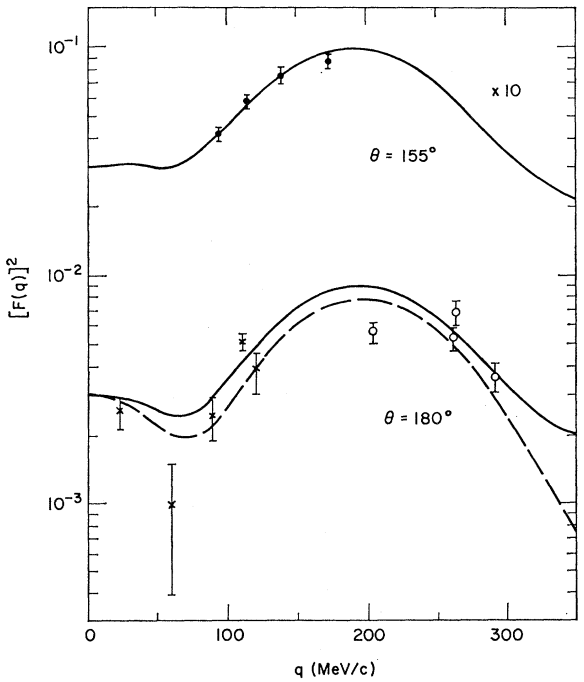

FIG. 14. The giant-resonance-region form factor at $\theta=155°$ and $\theta=180°$. The solid curves show the sum of the discrete ($1^-+1^-+2^-$) and the quasielastic contributions and the dashed curve the discrete contribution only. The data shown are ○ Ref. 8, **x** Refs. 17 and 26, and ● Ref. 19 (integrated between $\omega=21$ MeV and $\omega=27$ MeV). From Ref. 8 there is one extra datum at 350 MeV/c which is too low to be plotted in this figure.

This relatively simple calculation of the nonresonant quasielastic contribution to the cross section could be improved in a straightforward way by using a more realistic nuclear potential, say a Woods-Saxon potential with spin-orbit splitting. The inclusion of a Coulomb potential and a separate treatment of proton and neutron energies would be more realistic as well. A more difficult step would be to include configuration mixing in the continuum[32] over a large range of momentum transfers; another would be a proper treatment of the c.m. correction.[23] In this calculation, the difficult problem of treating the c.m. correction has been all but ignored and we have simply used the harmonic-oscillator correction $g_{\text{c.m.}}(q^2)$ given in Eq. (15). The results are not significantly changed if this correction is omitted (e.g., at $q=500$ MeV/c the c.m. correction increases the calculated cross section by only a factor of 2). However simplified the model is, we conjecture that it at least incorporates the main features of particle-hole states in a finite potential well. A more detailed account of this quasielastic calculation particularly at high excitation energies will be reported in the near future.

To the quasielastic form factor are added the form factors of the two 1^- states and the 2^- state in the giant resonance region (all calculated using harmonic-oscillator wave functions). The two 1^-, $E1$ form factors are shown in Fig. 12. At small values of q (and consequently in photoexcitation which is on mass shell) the $(1p_{3/2})^{-1}(1d_{5/2})$-dominated form factor is the important one. At higher q, however, the $(1p_{3/2})^{-1}(1d_{3/2})$-dominated spin-flip form factor becomes generally more important, particularly around 200 and beyond about 400 MeV/c. The two are of equal magnitude at about 80 MeV/c. Lewis and Walecka[6] have also considered the Goldhaber–Teller model of pure charge oscillations and the Steinwedel–Jensen hydrodynamical model of the giant resonance and have shown that for these models the form factor continues to fall with increasing momentum transfer beyond 80 MeV/c, whereas the data and the particle-hole form factors both rise.

The longitudinal $C1$ contributions are found to be significant only at small values of q where they fill in the diffraction minimum at $q\sim80$ MeV/c obtained with just the $E1$ form factors. Following the argument put forward in LW the longitudinal $C1$ form factors (the amplitudes squared) have been reduced by a factor of 2. In fact, data[19] obtained at $q=93$ MeV/c and different angles yield a longitudinal form factor which is consistent with the calculated value where the calculated $C1$ form factors are reduced by the factor of 2. Including the 2^- in the giant resonance region makes only a little difference, its main effect being to fill in the diffraction minimum in the dipole form factor which occurs between 300 and 400 MeV/c.

The total discrete form factor (the sum of the two 1^- and the 2^- form factors) is shown in Fig. 13 (dashed curve) along with the sum of this discrete form factor and the quasielastic form factor. The latter is compared with the data of Sick and Hughes[3] in Fig. 13. The general agreement between calculated and experimental form factors is seen to be reasonably good. As with all the other complexes considered here, the high q fall off is where the agreement is poorest. The relative importance of discrete and quasielastic contributions to the cross section is particularly striking: At low q the discrete form factor is much larger than the quasielastic form factor, while at high q their roles are reversed.

The 3^- discrete form factor was not included in this calculation as it was felt that, on the basis of Friar's continuum-model calculation[32] where the 3^- was found to be broad and to peak at about $\omega=27$ MeV, it would contribute mainly at higher excitation energies than those considered here (21–27 MeV). At low momentum transfer, this 3^- form factor is relatively small, having only comparable amounts of longitudinal and transverse strength. However, at momentum transfers beyond about 300 MeV/c the 3^- form factor is relatively large and fills in the diffraction dip in the total form factor which occurs between 300 and 400 MeV/c. Indeed if only part of the 3^- contribution is included (with the remainder of its strength lying at higher excitation

energies), then excellent agreement with the data of Sick and Hughes can be obtained up to $q\sim500$ MeV/c.

Finally, in Fig. 14 the giant resonance region form factor is compared with data[8,17,19,20] taken at $\theta=155°$ and 180°. The solid curves include both the quasi-elastic and discrete (dipole and quadrupole) form factors and the dashed curve the discrete form factor only.

IV. DISCUSSION

In summary, we have considered the $T=1$, single-particle-hole states in C^{12} on the basis of the particle-hole formalism of Lewis and Walecka,[6] using harmonic-oscillator wave functions for basis states. As in the calculation of Lewis and Walecka the pure j-j coupled particle-hole states here were mixed by a residual interaction, taken to be a Serber-Yukawa force with parameters obtained by fitting low-energy n-p scattering data.[7] The resulting energy spectrum contains groups of states which can be identified with the gross features excited in electron scattering: a 1^+ at 15.1 MeV, a 16-MeV complex $(2^+, 2^-)$, a 1^- at 18.1 MeV, a 19-MeV complex $(2^+, 2^-)$, a 1^- at 18.1 MeV, a 19-MeV complex $(2^-, 3^-, 4^-)$, and a giant resonance $(1^-, 1^-, 2^-)$. These complexes of neighboring single-particle-hole states are taken to be the doorway states for electroexcitation and yield inelastic-electron-scattering form factors to be compared with experimental data averaged over energy intervals on the order of 1 MeV.

The positions of the levels obtained are within a few MeV of their experimental energies (where known), being the worst for the 1^+–2^+ doublet where intermediate coupling can be important.[30] A different spin-dependent force can improve the agreement here and, in particular, place the doublet in the experimental order (rather than inverted as with the Serber-Yukawa force). The odd-parity states are found to be generally about an MeV too high in energy when the Serber-Yukawa force is used. Notably, the lowest-lying 1^- and 2^- states [those dominated by the $(1p_{3/2})^{-1}(2s_{1/2})$ pure particle-hole state] are the furthest from their experimental energies. However the states in the giant resonance region are clearly grouped as are the states in the 19-MeV complex, where, in particular, the 2^- and the unobserved 4^- states are found to be within a few hundred keV.

Good agreement is obtained for the momentum-transfer dependence of the form factors for these complexes when compared with energy-averaged experimental data. The amplitudes of the transitions to the 1^+ and 2^+ states had to be reduced by a factor of 2, indicating that the simple particle-hole model is inadequate; however, the q dependence is reproduced qualitatively, particularly in predicting a diffraction minimum in the $M1$ form factor. The form factors for the odd-parity particle-hole states are in reasonable agreement in amplitude with experiment and need at most a reduction factor of $\sqrt{2}$ to yield excellent agreement. Factors of this order result from treating the whole problem to a higher order, for instance by considering 2p-2h states as well as 1p-1h states[35] or by using the random-phase approximation to obtain higher configurations.[36] In any case, the momentum-transfer dependence is in good agreement with experiment up to 400–500 MeV/c. For higher momentum transfers, the calculated form factors decrease too rapidly with increasing q, a characteristic of the Gaussian-like harmonic-oscillator wave functions. This high-q dependence may be improved, as it is in the case of the elastic form factor,[27] by using finite-well wave functions. The fact that the behavior of both elastic and inelastic form factors can be at least qualitatively explained at high momentum transfer, where hard-core-induced correlations are expected to have an effect,[37] implies that at present the existence of such correlations cannot unambiguously be inferred from the experimental data.

In conclusion, good agreement is obtained in comparing the form factors for groups or complexes of single-particle-hole states with the gross structure seen experimentally in electroexcitation. This is a powerful means for locating and studying the collective particle-hole structure, particularly at high momentum transfer where the structure is relatively simple with only a few strongly excited features and where states of high angular momentum can easily be reached.

ACKNOWLEDGMENTS

It is a pleasure to thank Professor J. D. Walecka for many helpful discussions during the course of this work and to thank Dr. I. Sick and Dr. E. B. Hughes for an enjoyable and fruitful collaboration. Furthermore, the author wishes to express his thanks to Professor L. I. Schiff for extending the hospitality of the Institute of Theoretical Physics.

APPENDIX

For completeness, the matrix elements of the multipole operators [Eq. (16)–(18)] reduced in angular momentum and isospin are tabulated here. Radial matrix elements of the spherical Bessel functions for harmonic-oscillator wave functions are obtained using expressions given by deForest and Walecka.[2] Here we have $T=1$ and so have only the isovector magnetic moment μ_V. With $y=(bq/2)^2$, the polynomials $p_{C\mathcal{L}}(y)$, $p_{E\mathcal{L}}(y)$, and $p_{M\mathcal{L}}(y)$ for multipolarity $\mathcal{L}$ are defined by setting

[35] G. E. Walker, Phys. Rev. **174,** 1290 (1968).
[36] V. Gillet and M. A. Melkanoff, Phys. Rev. **133,** B1190 (1964).
[37] W. Czyż and K. Gottfried, Ann. Phys. (N.Y.) **21,** 47 (1963).

the reduced matrix elements[38] equal to

$$(n_1(l_1\tfrac{1}{2})j_1 :: \hat{M}_{\mathcal{L}}^{\mathrm{Coul}} :: n_2(l_2\tfrac{1}{2})j_2) = (3/4\pi)^{1/2}[1+(q_\mu^2/8M^2)(1-2\mu_V)]y^{\mathcal{L}/2}e^{-y}p_{C\mathcal{L}}(y)$$

for Coulomb multipoles, (26)

$$(n_1(l_1\tfrac{1}{2})j_1 :: \hat{T}_{\mathcal{L}}^{\mathrm{el}} :: n_2(l_2\tfrac{1}{2})j_2) = (3/4\pi)^{1/2}(1/bM)y^{(\mathcal{L}-1)/2}e^{-y}p_{E\mathcal{L}}(y) \quad \text{for electric multipoles,} \tag{27}$$

and

$$(n_1(l_1\tfrac{1}{2})j_1 :: i\hat{T}_{\mathcal{L}}^{\mathrm{mag}} :: n_2(l_2\tfrac{1}{2})j_2) = (3/4\pi)^{1/2}(1/bM)y^{\mathcal{L}/2}e^{-y}p_{M\mathcal{L}}(y) \quad \text{for magnetic multipoles.} \tag{28}$$

Note the extra factor $1/(bM)=(\omega_0/M)^{1/2}$ in the transverse form factors, producing a different dependence on the oscillator parameter for longitudinal and transverse form factors.

The polynomials $p_{C\mathcal{L}}(y)$, $p_{E\mathcal{L}}(y)$, and $p_{M\mathcal{L}}(y)$ contain only non-negative powers of y and consequently at small momentum transfer the leading terms vary as $y^{\mathcal{L}/2}$, $y^{(\mathcal{L}-1)/2}$, and $y^{\mathcal{L}/2}$, respectively. For example, only $C0$ and $E1$ form factors can be finite at $q=0$. In fact, for some particle-hole combinations the constant term in the polynomial may vanish and the leading term may vary as some higher power of y (see for example the $E2$ term below). For the particle-hole states involved in the present work, these polynomials are explicitly

$(1p_{1/2})(1p_{3/2})^{-1}$:

1^+, $p_{M1}(y)=\frac{2}{3}[1+\mu_V(-2+y)]$,

2^+, $p_{C2}(y)=(2\sqrt{2}/3)$, $p_{E2}(y)=-(2\sqrt{3}/3)\mu_V y$.

$(2s_{1/2})(1p_{3/2})^{-1}$:

1^-, $p_{C1}(y)=(2\sqrt{2}/3)(1-y)$, $p_{E1}(y)=-\frac{2}{3}[(1+y)+\mu_V(y-y^2)]$,

2^-, $p_{M2}(y)=-(2\sqrt{3}/3)\mu_V(1-y)$.

$(1d_{5/2})(1p_{3/2})^{-1}$:

1^-, $p_{C1}(y)=2(1-\frac{2}{5}y)$, $p_{E1}(y)=-\sqrt{2}[(1-\frac{4}{5}y)+\mu_V(-y+\frac{2}{5}y^2)]$,

2^-, $p_{M2}(y)=-(2/15)(70)^{1/2}[1+\mu_V(\frac{3}{2}-\frac{5}{7}y)]$,

3^-, $p_{C3}(y)=-(4/15)(6)^{1/2}$, $p_{E3}(y)=(4/15)\sqrt{2}(1-\frac{1}{2}\mu_V y)$,

4^-, $p_{M4}(y)=(2/7)(14)^{1/2}\mu_V$.

$(1d_{3/2})(1p_{3/2})^{-1}$:

1^-, $p_{C1}(y)=-\frac{2}{3}(1-\frac{2}{5}y)$, $p_{E1}(y)=(\sqrt{2}/3)[(1-\frac{4}{5}y)+\mu_V(4y-(8/5)y^2)]$,

2^-, $p_{M2}(y)=(2/15)(30)^{1/2}(1-\mu_V)$,

3^-, $p_{C3}(y)=\frac{4}{5}$, $p_{E3}(y)=-(4/15)\sqrt{3}(1+2\mu_V y)$.

$(1p_{1/2})(1s_{1/2})^{-1}$:

1^-, $p_{C1}(y)=-(6^{1/2}/3)$, $p_{E1}(y)=(\sqrt{3}/3)(1+2\mu_V y)$.

The form factors for the states involved here are then obtained by taking linear combinations of these polynomials for a given multipole with the mixing coefficients given in Table I.

[38] The reduction in isospin simply contributes a factor $1/\sqrt{2}$.